Analysing laser machined YBCO micro bridges using Raman spectroscopy and transport measurements aiming to investigate process induced degradation

K. LANGE[1], M. SPARKES[1,*] J. BULMER[2], J.P.F. FEIGHAN[2], W. O'NEILL[1], T.J. HAUGAN[3]

[1]*Institute forManufacturing, University of Cambridge, United Kingdom*

[2]*Department of Materials Science & Metallurgy, University of Cambridge, United Kingdom*

[3]*AFRL/RQQM, US Air Force Research Lab, Wright Patterson AFB, OH, United States*

*Corresponding author e-mail: mrs46@cam.ac.uk

ABSTRACT

Machining high temperature superconducting (HTS) thin films is challenging due to the material's sensitivity. Here, 200 nm thick YBCO micro bridges were machined with a femtosecond laser (300 fs, @ 1030 nm) as a chemical free and flexible method with minimal edge damage. Transport measurements and Raman spectroscopy were used to analyse the bridges before and after laser processing. While transport and Raman measurements are commonly used separately to evaluate YBCO, our approach links both techniques to analyse laser induced damage. The link between changes in the Raman spectrum and transport measurements is investigated by identifying changes caused by repeated heat treatments while sequentially measuring the critical current density (J_c) and Raman spectra. The data obtained is used to predict J_c losses from changes in Raman peak intensities and shifts. This technique is further investigated by applying it to laser machined YBCO bridges which were exposed to highly localised heating. Results show that for bridge widths of 10 µm, a femtosecond laser can be used to repeatedly successfully machine bridges with no loss in J_c and that there is some correlation to I_c changes in the Raman spectra.

Keywords: Femtosecond laser; micro machining; $YBa_2Cu_3O_{7-x}$ thin films; heat treatments; transport measurements; Raman spectroscopy

1. INTRODUCTION

Since their discovery, high temperature superconductors (HTS) have been used in various applications such as microwave filters, antennas, single photon bolometers and more [1], [2]. The most researched HTS is $YBa_2Cu_3O_{7-x}$ due to its high critical temperature (< 90 K). Most applications require patterning of YBCO on a micro/nano scale, however, this proves to be very challenging due to the material's sensitivity, since the superconductivity is easily lost by heat degradation, chemical interaction, electron/ion irradiation and humidity [3]-[6]. Current machining

techniques are lithography (wet and dry) [7], [8], Focused Ion Beam (FIB) [9], [10], and laser machining (< fs) [9]. While lithography is comparably quick, it does not allow much design freedom as a new mask would be required for each design change. Another disadvantage is the degrading effect on YBCO caused by chemicals and/or electron beams used in Lithography.. FIB machining has a high design resolution and flexibility as the design can be easily changed using CAD software, with helium FIBs achieving nm feature sizes [10]. FIBs have two major disadvantages, one being the very limited processing speed and the other being ion implantations, which alter the crystal structure of YBCO leading to degradation. While laser machining offers the advantages of design flexibility and high processing speed, the challenge of controlling heat input requires consideration. For this work, an ultrafast laser (SATSUMA; Amplitude Systèmes) was used, operating at a wavelength of 1030 nm and a pulsewidth of 300 fs to machine YBCO micro bridges to different widths. The laser gives limited thermal effects due to direct solid-vapour transitions. To evaluate the effects of the laser on YBCO, transport and Raman measurements were conducted. While transport measurement is the most common technique to evaluate HTS, Raman spectroscopy is added as a quick and non-contact measurement procedure to assess thermal damage which result in oxygen diffusion. Depending on the oxygen content of YBCO, the vibrational modes and their respective Raman peaks of the different atoms change [11], [12]. Since laser machining has several variables that could influence the Raman spectrum, YBCO thin films were also heated and measured as a reference.

2. EXPERIMENTAL SETUP

YBCO (M-type) films of 200 nm thickness were grown on MgO substrate in a bridge arrangement by STAR Cryoelectronics LLC (Santa Fe, NM, US). Individual samples were composed of five bridges with 20 nm thick gold contacts, see Figure 1. Heat treatments were conducted at room temperature in air. A hot plate was set to a temperature of 300 °C and the sample heated for 10 s. Laser machining was conducted using the setup shown in Figure 2. The YBCO bridges were processed under ambient conditions with the laser parameters listed in Table 1. The sample was mounted on a stage which has an accuracy of ± 3 µm in X/Y direction and ± 0.5 µm in Z direction. To correct tip/tilt, an additional stage was mounted on the CNC stage. An objective (NA = 0.35) (12OI09; COMAR Optics) with a focal length of 12.7 mm focussed the laser beam to a theoretical $1/e^2$ spot diameter of 4.58 µm. To improve the machining edge quality, a beam shaper (Focal-πSaper 9_1064; AdlOptica) was added to the setup to change the Gaussian beam profile to a flat top. The transport and Raman properties of the YBCO samples were measured before and after heat/laser experiments.

3. RESULTS AND DISCUSSION

3.1. Laser ablation

After processing YBCO thin films with a range of pulse energies (36.7 nJ – 282 nJ), repetition rates and processing speeds, a pulse energy of 215 nJ at 1 kHz was determined to be optimum to machine YBCO bridges in one pass at 1 mm/s while avoiding damage to the MgO substrate. The bridges were machined from one side only including a 50 µm radius to avoid current crowding. A comparison between the edges made by lithography and laser machining is shown in Figure 3. The RMS edge roughness for the lithography edge is 0.955 µm with a peak-to-peak roughness of 3.43 µm. The RMS edge roughness of the laser-processed sample is comparable to the lithography value of 0.957 µm. The peak-to-peak value is slightly higher at 4.19 µm.

3.2. Transport measurements

A four-point probe cooled in liquid nitrogen was used for the transport measurements. Spring-loaded pogo pins were connected to the gold pads using indium to increase the contact area. Current pulses from a source meter (2440; Keithley) were sent through the sample while the voltage was measured by a nano voltmeter (2182; Keithley). To determine the critical current a criterion voltage of 0.5 µV was used. During the heat treatments, a 10 µm YBCO bridge sample was repeatedly measured. The decline of the critical current with each heat treatment (10 s at 300 °C) is shown in Figure 4.

3.3. Raman spectroscopy

A Raman microscope (Senterra; Bruker) was used with an excitation wavelength of 532 nm and a 20X objective. At 532 nm the optical penetration depth of YBCO is 70-80 nm [13], approaching half the film thickness. The measurements were taken with 5 mW laser power over 10 s with 3 acquisitions over one data point with a spot size of < 4 µm. As stated in [13], once YBCO has been degraded, the Cu2 peak intensity surpasses the Ba peak as a result of oxygen loss during the phase transition from the orthorhombic (superconducting) to the tetragonal (insulating) crystalline structure of YBCO, see Figure 5. In this study, the Raman peak intensity change during the heat treatments was further analysed by relating Ba/Cu2 ratios to transport measurement results, see Figures 6 and 7. With the decline of the Ba/Cu2 ratio, the critical current of the sample also decreased. Based on repeated heat treatment experiments, it appears that for this work, below a Ba/Cu2 ratio of 1.15, the YBCO sample is more likely to have lost its superconductivity. Laser machined bridges were also examined using Raman to identify laser induced damage and possible heat influences. Spectra from laser machined bridges are shown in Figure 8. Bridge 1 was machined from 100 µm to ~ 30 µm and the Raman spectra show slight

changes in the peak intensities, especially a decrease in Ba. The width of Bridge 2 was reduced from 100 µm to ~ 10 µm and the Raman spectra show a significant change in the Ba/Cu2 ratio, similar to the changes observed during the heat treatments. This suggests that the sample has degraded, confirmed by transport measurements. More laser machined bridges were inspected with Raman spectroscopy to investigate whether these spectral changes are repeatable, see Figure 9. The Raman intensity for both bridges changed after the laser process. The Ba/Cu2 ratio decreased from 1.25 to 1.18 for Bridge 2 (4 % J_c decrease) and from 1.27 to 1.18 for Bridge 3 (12 % Jc decrease). Similar to the heat treatment results, the Ba/Cu2 ratio decreased with decreasing current density. Yet, during the heat treatments, a Ba/Cu2 ratio of 1.18 already showed an 83 % J_c decrease compared to a J_c decrease of 4 % to 12 % when using the laser. Laser machining is a far more complex process than the heat treatments. These results let us assume that the Ba/Cu2 ratio can give us some information about the state of a bridge after the laser process and that the bridges seem to have suffered from only limited heat effects. Defects (e.g. structural) might also play another role in terms of possible degradation sources.

4. CONCLUSION

In these experiments, a link between Raman spectroscopy and transport measurements was investigated. A decreasing Ba/Cu2 ratio indicates a decreasing current density. With this ratio, Raman spectroscopy could have the potential to be used as a new inline measurement method to monitor the degradation of YBCO bridges. Comparing the results from heat treatments and laser machining, similarities between Ba/Cu2 ratios and critical current density were observed. The laser process introduces more variables that could be a degradation source than simple heat treatments. Raman measurements for laser machined samples are also limited by the Raman spot size and the position accuracy of the respective sample stage.

ACKNOWLEDGEMENTS

This work was partially supported by the Air Force Research Laboratory - Aerospace Systems Directorate (AFRL/RQ), the Air Force Office of Scientific Research (AFOSR) under contract LRIR #18RQCOR100, and AFOSR/EOARD under contract FA 16I0E050 and the EPSRC (grant number: EP/L016567/1).

NOMENCLATURE

I_c	critical current (A)
J_c	critical current density (MA/cm²)

REFERENCES

[1] Aghabagheri S., Rasti M., Mohammadizadeh M.R., Kameli P., Salamati H., Mohammadpour-Aghdam K. and Faraji-Dana R. High temperature superconducting YBCO microwave filters. *Physica C: Superconductivity and its Applications* **549** (2018), 22–26.

[2] Curtz N., Koller E., Zbinden H., Decroux M., Antognazza L., Fisher Ø. and Gisin N. Patterning of ultrathin YBCO nanowires using a new focused-ion-beam process. *Supercond. Sci. Technol.* **23**, (2010), 045015.

[3] Nawaz S., Arpaia R., Lombardi F. and Bauch, T. Microwave Response of Superconducting Y Ba 2 Cu 3 O 7 − δ Nanowire Bridges Sustaining the Critical Depairing Current: Evidence of Josephson-like Behavior. *Physical Review Letters* **110**, (2013).

[4] Quere, Y. (1989). *Irradiation damage in superconductors*. Retrieved 10th January 2018, from http://inis.iaea.org/Search/search.aspx?orig_q=RN:21039530

[5] Ballentine P. H., Kadin A. M., Fisher M. A., Mallory D. S. and Donaldson, W. R. Microlithography of high-temperature superconducting films: laser ablation vs. wet etching. *IEEE Transactions on Magnetics* **25**, (1989), 950–953

[6] Arpaia R., Nawaz S., Lombardi F. and Bauch, T. Improved Nanopatterning for YBCO Nanowires Approaching the Depairing Current. *IEEE Transactions on Applied Superconductivity* **23**, (2013), 1101505–1101505.

[7] Lee S.-G., Oh S.-H., Kan, C. S. and Kim, S.-J. Superconducting nanobridge made from YBa2Cu3O7 film by using focused ion beam. *Physica C: Superconductivity* **460–462, Part 2**, (2007), 1468–1469.

[8] Wu C. H., Jhan F. J., Chen J. H. and Jeng, J. T. High- T c Josephson junctions fabricated by focused ion beam direct milling. *Supercond. Sci. Technol.* **26**, (2013), 025010.

[9] Hix K. E., Rendina M. C., Blackshire J. L. and Levin, G. A. (2004). *Laser Micromachining of Coated YBa2Cu3O6+x Superconducting Thin Films*. Retrieved 18th October 2016, from http://arxiv.org/abs/cond-mat/0406311

[10] Cybart S. A., Cho E.Y., Wong T.J., Wehlin B.H., Ma M.K., Huynh C. and Dynes R.C. Nano Josephson superconducting tunnel junctions in YBa2Cu3O7–δ directly patterned with a focused helium ion beam. *Nat Nano* **10**, (2015), 598–602.

[11] Maroni V. A., Reeves J. L. and Schwab G. On-line Characterization of YBCO Coated Conductors Using Raman Spectroscopy Methods. *Appl. Spectrosc., AS* **61**, (2007), 359–366.

[12] Iliev M. N., Hadjiev V. G. and Ivanov V. G. Raman Spectroscopy of Local Structure and Reordering Processes in YBa2Cu3O7-δ-Type Compounds. *J. Raman Spectrosc.* **27**, (1996), 333–342.

[13] Li Y. B., Shelley C., Cohen L.F., Caplin A.D., Strading R.A., Kula W., Sobolewski R. and MacManus-Driscoll J.L. Raman studies of laser-written patterns in YBa2Cu3Ox films. *Journal of Applied Physics* **80**, (1996), 2929–2934.

[14] Maroni V. A., Reeves J. L. and Schwab G. On-line Characterization of YBCO Coated Conductors Using Raman Spectroscopy Methods. *Appl. Spectrosc., AS* **61**, (2007), 359–366.

[15] Venkataraman K., Baurceanu R. and Maroni V.A. Characterization of MBa2Cu3O7-x Thin Films by Raman Microspectroscopy. *Appl Spectrosc* **59**, (2005), 639–649.

FIGURES AND TABLES

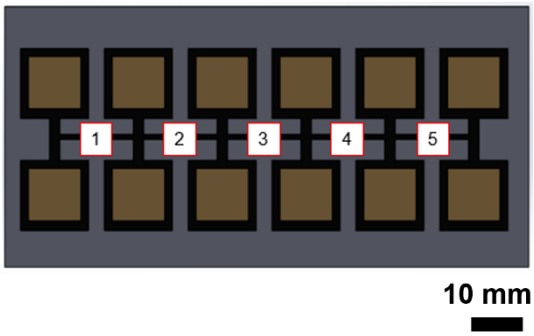

FIGURE 1 Schematic of one YBCO sample with 5 bridges (numbered).

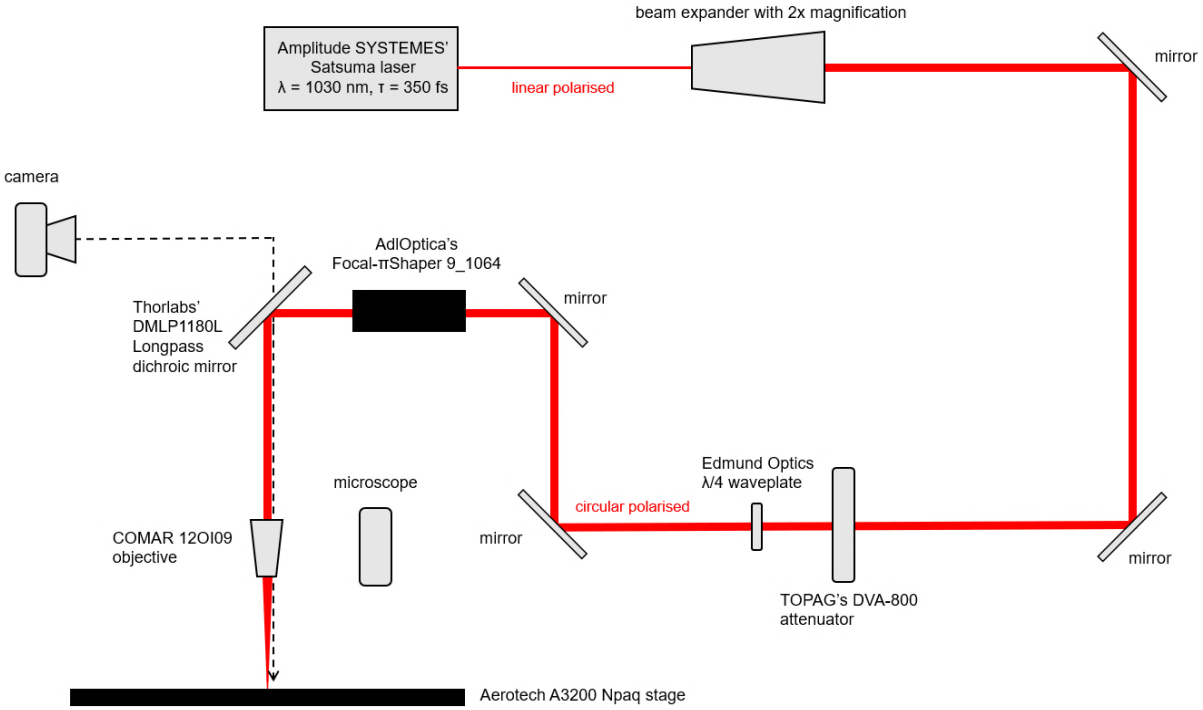

FIGURE 2 Experimental setup of the laser platform.

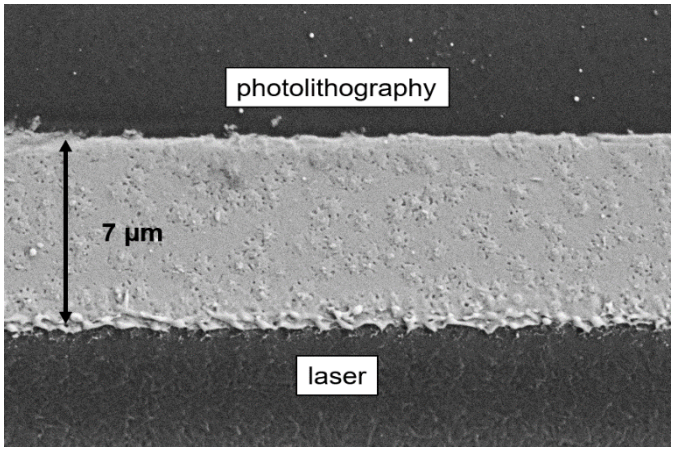

FIGURE 3 A 30 µm YBCO bridge machined to 7 µm. Both the photolithography and the laser edge are visible.

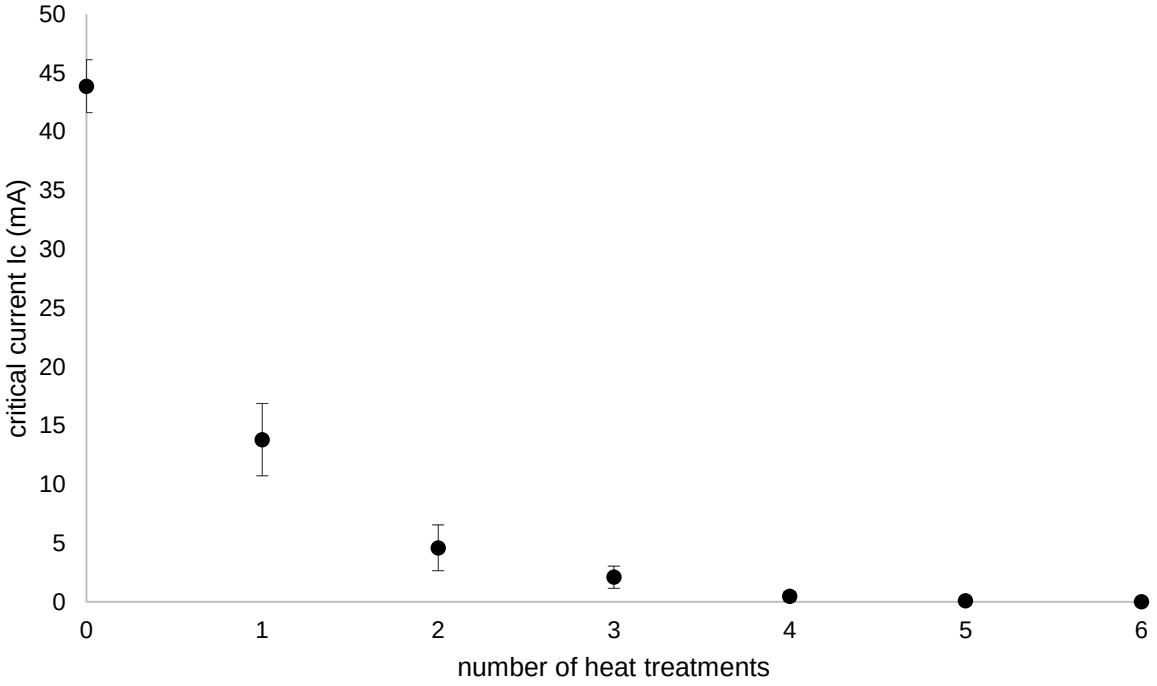

FIGURE 4 Critical current decrease over multiple heat treatments of a 10 µm YBCO bridge sample. The error for the critical current is 140 µA at a criterion voltage of 0.5 µV.

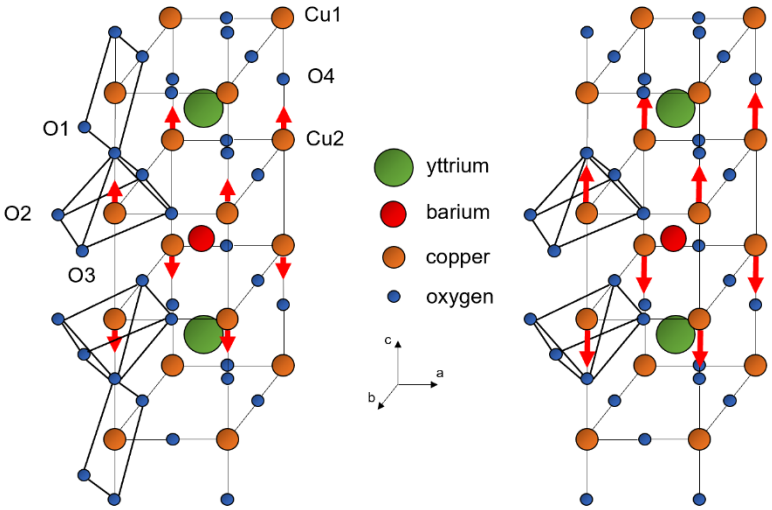

FIGURE 5 Crystalline structure of YBCO. The schematic on the right shows the orthorhombic structure of YBCO (superconducting) while on the left the tetragonal structure (insulating) is shown. The red arrows are indicating the Cu2 vibrational mode which is detected by Raman spectroscopy. The direction of the vibrational modes is further explained in reference [15].

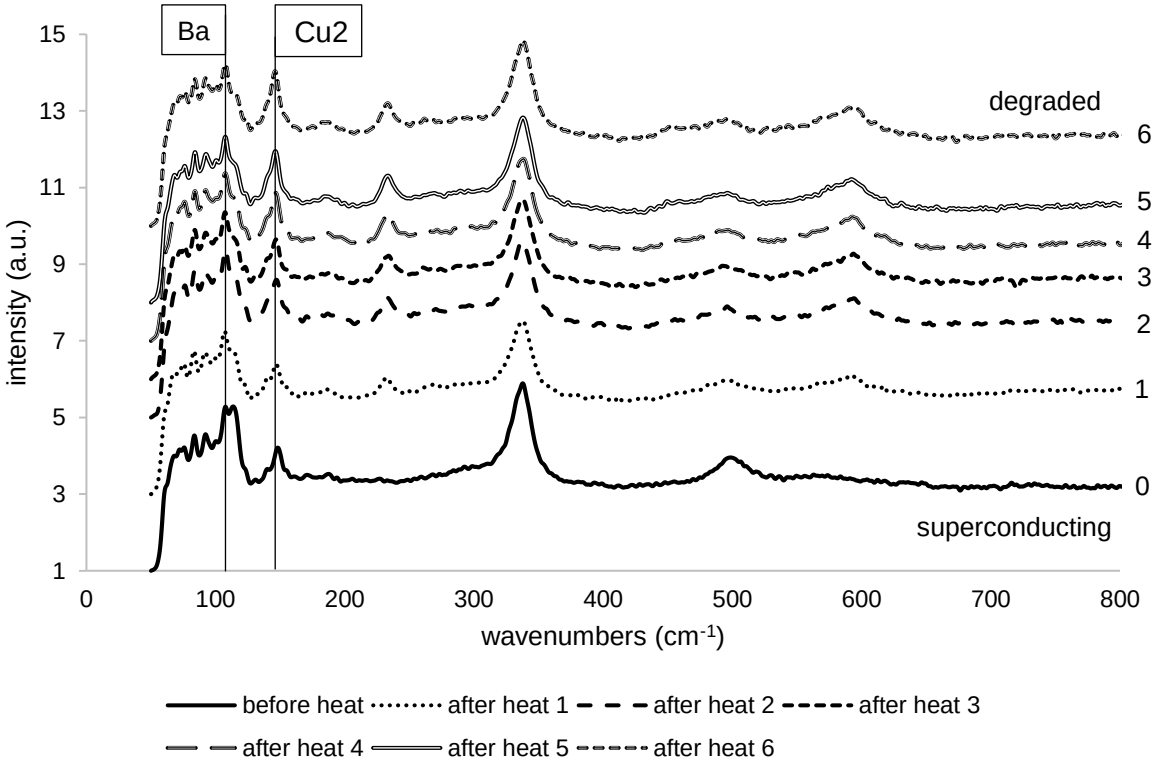

FIGURE 6 Changes in the Raman spectra are observed as the sample changes from superconducting to complete degradation. The different spectra are displayed with an offset to better distinction of the changes.

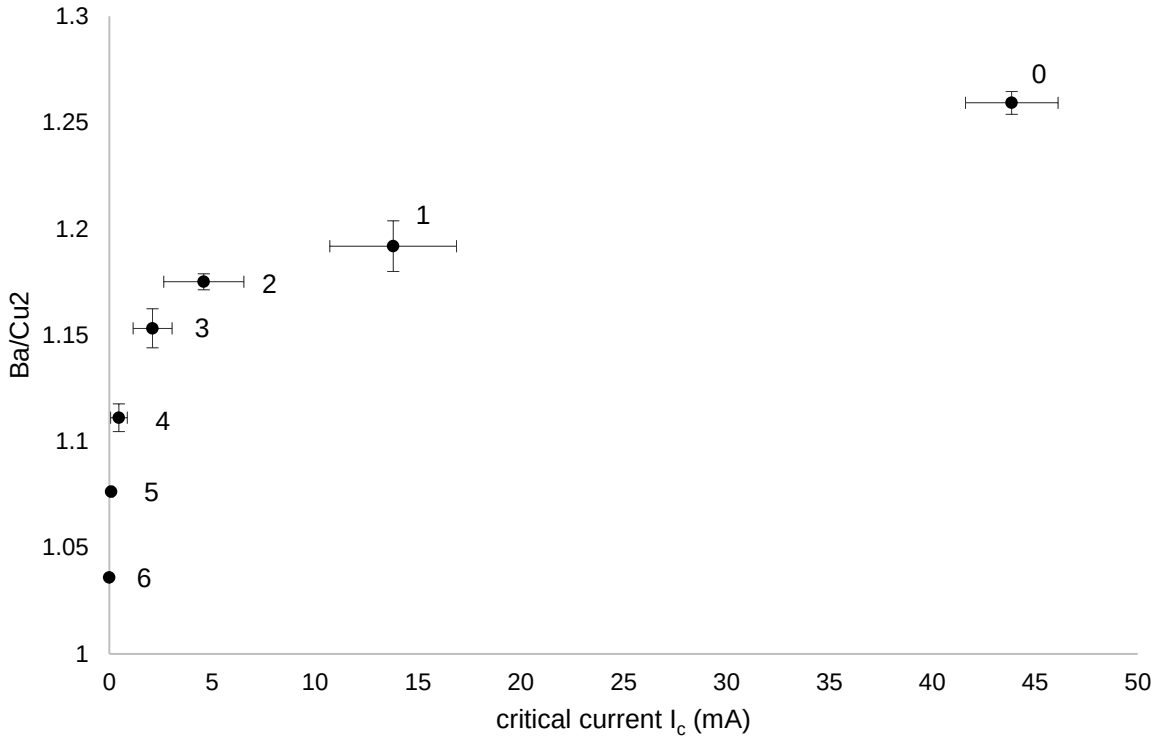

FIGURE 7 Ba/Cu2 ratio vs critical current measured before and after heat treatments.

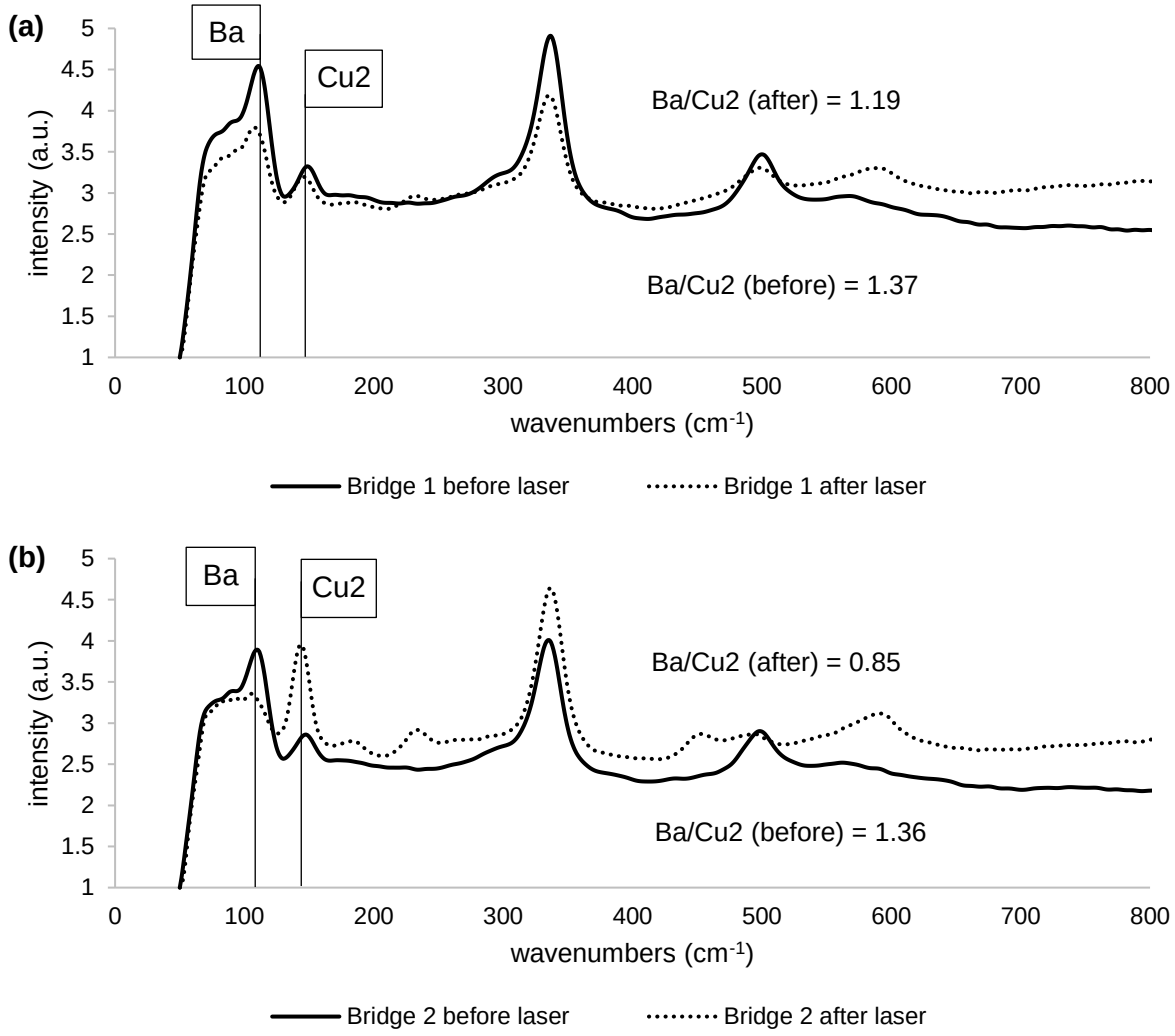

FIGURE 8 Raman spectra before and after the laser machining of two bridges (a), (b).

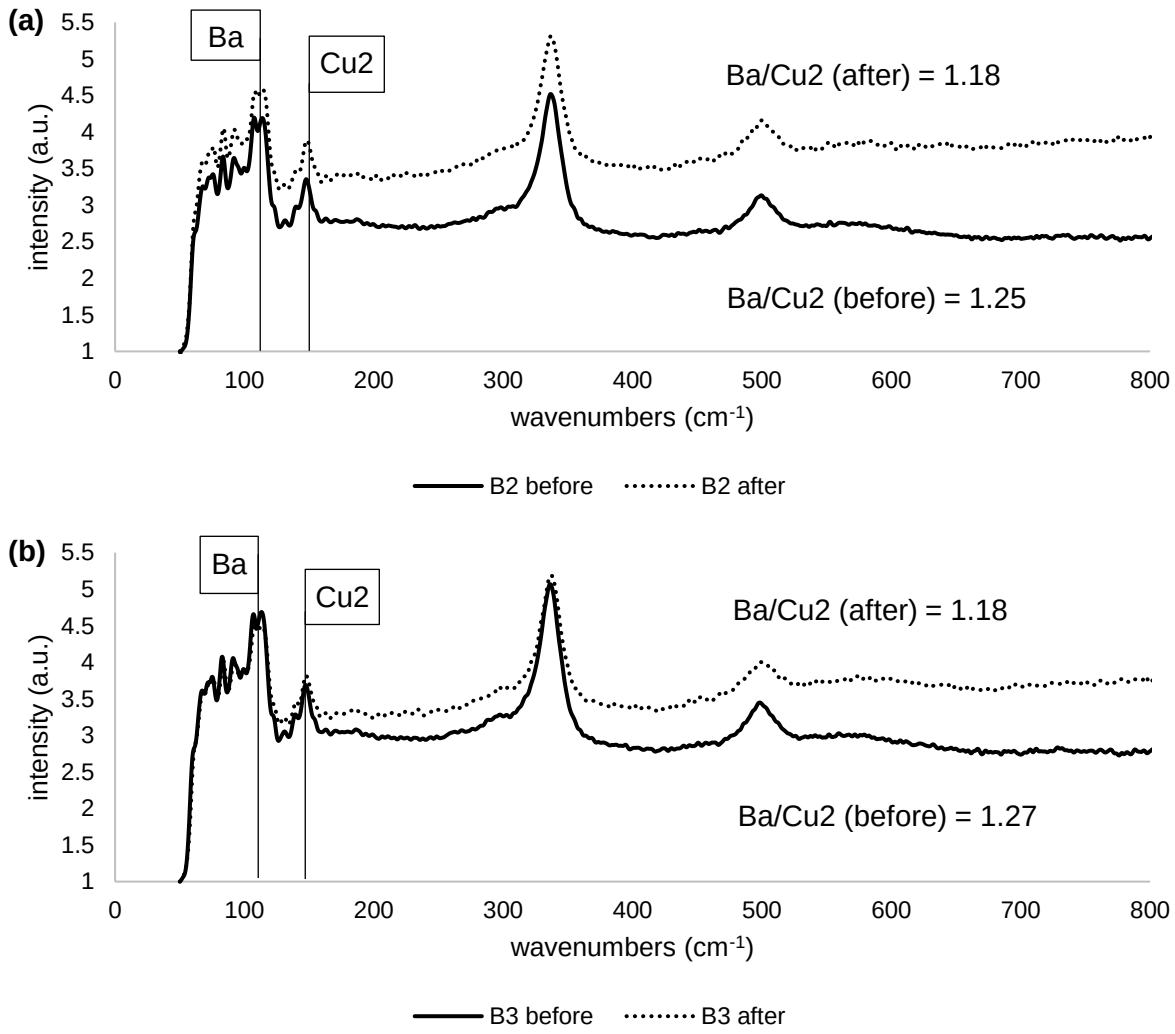

FIGURE 9 Two bridges were machined from 30 µm to 15 µm (a) and 6.8 µm (b). They were machined at 1 kHz with a processing speed of 1 mm/s.

TABLE 1
Satsuma laser parameters.

Laser model	**Amplitudes Systèmes Satsuma**
Wavelength	1030 nm
Pulse duration	~ 300 fs
Pulse repetition rate	1-2000 kHz
Raw beam diameter	2.0 ± 0.5 mm
M^2	1.1